Solubility of Solid Polycyclic Aromatic Hydrocarbons in Pressurized Hot Water at Temperatures from 313 K to the Melting Point

Pavel Karásek, Josef Planeta, and Michal Roth*

Institute of Analytical Chemistry, Academy of Sciences of the Czech Republic, Veveří 97, 61142 Brno, Czech Republic

Aqueous solubilities of two- to four-ring solid polycyclic aromatic hydrocarbons (PAHs) (naphthalene, anthracene, 1,2-benzanthracene, triphenylene, and *p*-terphenyl) were measured at temperatures within 313 K to the PAH melting point and pressures within the range (4 to 8) MPa by dynamic method combined with gas chromatography/ mass spectrometry. A novel feature of the apparatus was the use of a capillary restrictor to minimize the system volume downstream of the sampling point. The results for naphthalene and anthracene compare favorably with the literature data whereas the solubilities of 1,2-benzanthracene, triphenylene, and *p*-terphenyl in pressurized hot water are reported for the first time. The solubilities (equilibrium mole fractions, x_2) of PAHs are discussed in terms of temperature and hydrocarbon structure. Mean values of the relative change in the PAH solubility with temperature, $(\partial \ln x_2/\partial T)_\sigma$, range from 5.4×10^{-2} K^{-1} in naphthalene to 7.2×10^{-2} K^{-1} in *p*-terphenyl. The ln x_2 versus T plot for 1,2-benzanthracene is curved in the opposite direction as compared with the plots for anthracene, triphenylene, and *p*-terphenyl.

Introduction

Water is not only the greenest but also the most tunable of solvents, with different kinds of intermolecular interactions changing their relative importance as the temperature increases from the triple point to the critical point. Although the effects of temperature and pressure on the solvent properties and reactivity of water become most fascinating in the supercritical region,[1−6] important changes from the properties at ambient conditions can already be seen in liquid water at temperatures between the normal boiling point and the critical point.

The ever increasing emphasis on green, sustainable, environment- and resource-conscious procedures results in rising use of liquid water as a solvent or reaction medium. In analytical chemistry, for example, subcritical water extraction, also known as pressurized hot water (PHW) extraction, is now an established technique of sample treatment. Since its introduction,[7] the technique has seen relatively frequent applications compiled in several recent reviews.[8−10] Applications of PHW as a carrier fluid for chromatography also appear promising.[11] In addition, subcritical water has been used in environmental remediation applications to remove or decompose persistent pollutants such as pesticides[12,13] or polychlorinated biphenyls.[14] The interesting use of PHW to extract flavor and fragrance compounds from plant materials should also be noted.[15−17]

The relatively frequent applications of PHW contrast with scarce fundamental studies of aqueous solubilities of heavy organic compounds in a wide temperature range. Some of the studies focused on solubility of liquid organic compounds of application interest.[18−21] The aqueous solubility of solid organic compounds, while also very important in extractions and remediation applications, is a valuable source of fundamental information as it lends itself to an easier thermodynamic analysis as compared with the solubility of liquid organics. A major part of efforts to determine the solubilities of organic solids in PHW

were aimed at polycyclic aromatic hydrocarbons (PAHs). Rössling and Franck[22] employed UV spectrophotometry to determine the solubility of anthracene in several compressed solvents including PHW. A visual observation of solubility of heavy hydrocarbons (*n*-tetracosane, benzo[*e*]pyrene, *n*-nonadecylbenzene) and a white oil sample in near-critical water was reported by Sanders.[23] Later on, Miller and Hawthorne[24] developed an apparatus for production of saturated aqueous solution by passing PHW through a layer of solid solute mixed with an inert material, and Miller et al.[25] used the dynamic method to determine the solubilities of anthracene, pyrene, chrysene, perylene, and carbazole in PHW up to 498 K. Recently, Andersson et al.[26] reported solubilities in PHW of acenaphthene, anthracene, and pyrene at temperatures both below and above the melting points of the individual PAHs.

The purpose of this study is to complement the PAH in PHW solubility data with new information on solubility of solid PAHs. The results can be useful for the development of thermodynamic models of highly nonideal water (1) + PAH (2) systems as well as for the design of environmental remediation processes.

Experimental Section

Materials. Naphthalene (> 99 mol %), anthracene (99 mol %), 9,10-dimethylanthracene (99 mol %), *p*-terphenyl (> 99 mol %), 1,2-benzanthracene (99 mol %), triphenylene (98 mol %), and phenazine (dibenzopyrazine, 98 mol %) were purchased from Sigma-Aldrich (Prague, Czech Republic). As the analyses of the calibration solutions of these compounds by gas chromatography/mass spectrometry (GC/MS) did not indicate the presence of any major impurities, all compounds were used as received. Toluene (99.8 mol %) and methylene chloride (99.8 mol %) were obtained from Penta (Chrudim, Czech Republic). Water was purified with a reverse osmosis system Ultra Clear UV (SG Wasseraufbereitung und Regenerierstation GmbH, Barsbüttel, Germany). Glass beads (size (0.57 to 0.70) mm) used to prepare the packing of extraction cell were purchased from GlassDekorService (Valašské Meziříčí, Czech Republic). Before

* To whom correspondence should be addressed. E-mail: roth@iach.cz. Phone: +420 532 290 171. Fax: +420 541 212 113.
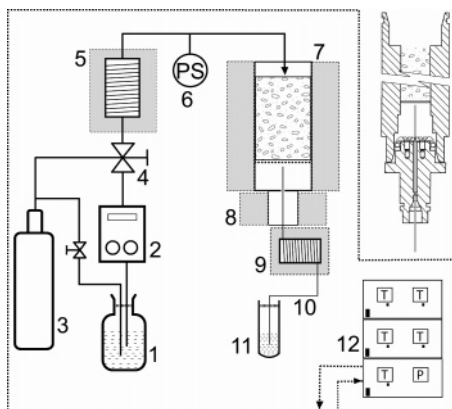
Figure 1. Schematic diagram of the extraction apparatus with a detail showing the extraction cell and the restrictor inlet assembly. Gray areas indicate the thermostated parts. 1, water reservoir; 2, HPLC pump; 3, helium tank; 4, main control valve; 5, preheater coil; 6, pressure sensor; 7, extraction cell housing; 8, restrictor inlet assembly housing; 9, restrictor heating drum; 10, sample collection vial; 11, fused-silica capillary restrictor; 12, temperature control units and pressure indication.

use, the beads were thoroughly rinsed with toluene and methylene chloride and then heated for 10 h to 523 K to remove any organic impurities.

Extraction Apparatus. A schematic diagram of the apparatus is shown in Figure 1. To prevent possible losses of the solute, care was taken to minimize the system volume downstream of the sampling point. The essential part of the setup was the flow-through extraction cell (length 110 mm, i.d. 4 mm, internal volume 1.4 cm^3) turned from nickel-based alloy Inconel 625. This alloy proved to be corrosion-resistant even when exposed to supercritical water.[27] The cell was housed in a vertical position within a massive aluminum block fitted with several platinum resistance thermometers and resistance heaters to ensure reliable calibration of the cell temperature and uniform heating of the cell. The block was encased in a heavy thermal insulation coat made from mineral wool packed in the annulus between the surface of the block and the outer aluminum cover. The lower part of the extraction cell contained a stainless steel mesh to support the cell packing (a mixture of the solid PAH with glass beads). Water in the reservoir flask was stripped off the dissolved air by bubbling a gentle stream of helium. Pure degassed water was fed to the cell through a preheater from a LC 1120 HPLC pump (GBC Scientific Equipment Pty Ltd., Dandenong, Victoria, Australia) operated in constant-flow rate mode. In the cell, saturated aqueous solution of the PAH studied was prepared by passing pure water through a 90-mm-long packed bed of a mixture of the crystalline PAH with glass beads. The aqueous solution left the cell through a piece of fused-silica tubing (length (120 to 130) cm, i.d. 75 μm, internal volume < 5.8 mm^3) serving as a flow restrictor, and it was collected in a 40-mL or 60-mL vial. Together with the water flow rate set by the pump, the length and diameter of the tubing controlled the extraction pressure. The restrictor inlet assembly fitted with a compression nut, and a Vespel/graphite ferrule was sealed to the lower part of the extraction cell. This arrangement made it possible to adjust the vertical position of the restrictor inlet (= the sampling point) to within (1 to 2) mm below the stainless steel mesh supporting the cell packing.

A major part of the length of the fused-silica restrictor was wound onto a 6 cm diameter heating drum turned from aluminum alloy. The temperatures of the restrictor inlet assembly and of the drum could be controlled independently of the extraction cell temperature, and they always exceeded the cell

temperature. This arrangement proved to be essential for correct operation of the device. The temperatures of all parts of the apparatus were controlled with four independent PID regulators (model 3116 temperature and process controller, Eurotherm Ltd., Worthing, West Sussex, U.K.). The standard uncertainty[28] in the measurement of the extraction cell temperature was ± 0.10 K. To prevent the capillary restrictor from getting plugged with the solid PAH nucleating from the aqueous solution, the temperature of the restrictor inlet assembly was adjusted to exceed the temperature of the extraction cell by 10 K. The temperature of the restrictor heating drum was always higher than the temperature of the restrictor inlet assembly, occasionally exceeding the PAH melting point by 15 K. During the solubility measurements, the average linear velocity of the aqueous effluent in the restrictor was always higher than 3 m·s^{-1}, minimizing the time allowed for nucleation of the solute inside the restrictor (< 0.43 s). The pressure at the inlet of the extraction cell was monitored with an Efector 500 pressure sensor (model PA9021, IFM electronic GmbH, Essen, Germany). The standard uncertainty in the pressure measurement was ± 0.1 MPa. The surfaces in contact with the flowing aqueous solution were glass, Inconel 625, and very small exposed areas of stainless steel (the mesh) and fused silica (the restrictor).

Procedure. Prior to the extraction run with every individual PAH, a sufficient amount of PAH was mixed with glass beads and loaded into the extraction cell. The cell was connected to the apparatus at room temperature, and the system was thoroughly flushed with helium. Then the apparatus was slowly pressurized with water at room temperature; the flow rate was adjusted to maintain the operating pressure of cca 5 MPa; and the system was slowly heated to $T = 313$ K, the lower temperature limit of this study. After stabilization of the temperature and pressure (approximately 20 min), the system was ready for sampling the aqueous effluent. Depending on the operating temperature and on the restrictor employed, the mass flow rate of water required to achieve the operating pressure of 5 MPa ranged within (0.010 to 0.017) g·s^{-1}.

To take a sample of the extractor effluent, the outlet end of the restrictor was temporarily submerged below the level of a small amount of water (4 g) in the collection vial. The presence of water at the start of collection was needed to prevent boiling of the restrictor effluent at elevated operating temperatures. The collection vial was capped with Teflon-lined silicone rubber cap punched with a short piece of PEEK tubing for easy insertion of the restrictor. Depending on the expected solubility of the PAH solute, the sample collection time was either (300 or 600) s. At a particular temperature and water flow rate, five samples were taken of the aqueous solution. After taking the five samples, the apparatus was adjusted to the next operating temperature, and 1200 s was allowed for stabilization of the temperature, pressure, and composition of the aqueous effluent.

The amount of a single sample of aqueous effluent ranged within (3 to 6) g, and it was determined by weighing the collection vial before and after collection (standard uncertainty ± 0.01 g). After cooling to room temperature, the vial was kept at 5 °C for 24 h to promote crystallization of the precipitated PAH. Then a pre-estimated amount of toluene ((2 to 35) g) was added into the vial to transfer the PAH solute to the toluene layer. With each sample collected, at least 72 h was allowed for equilibration. Several times during the equilibration period, the sample vial was vigorously shaken and then immersed into an ultrasonic bath (model Sonorex RK 52 H, Bandelin electronic GmbH, Berlin, Germany) for 600 s to create an emulsion and

to increase the interfacial contact area. After equilibration and phase separation, a defined amount ((0.0001 to 1) cm^3) of the toluene layer was withdrawn from the vial and added to 1 cm^3 of pure toluene, and a known amount of the standard compound was added to the solution. The resultant mixture was analyzed by GC/MS. The internal standard was selected so as to elute from the GC column with the retention time distinct from but close to that of the particular PAH. Phenazine was employed as the internal standard with naphthalene and anthracene while 9,10-dimethylanthracene was used with the other PAHs studied. With every PAH investigated, the series of calibration solutions with suitable PAH/standard ratios were prepared in toluene.

GC/MS Operating Conditions. The apparatus employed was a TraceGC gas chromatograph equipped with a RTX-5MS capillary column (5 % diphenyl−95 % dimethylsiloxane, 30 m × 0.25 mm i.d., polymer film thickness 0.25 μm, Restek, Bellefonte, PA). The column outlet was coupled to a PolarisQ mass spectrometer (TraceGC + PolarisQ, Thermo Finnigan, San Jose, CA). Helium (99.995 %, SIAD, Braňany u Mostu, Czech Republic) was employed as the carrier gas, and the ionization energy (EI mode) was 70 eV. Although the peak-area integration and the subsequent calculations were always based on the particular molecular ion to increase precision and to avoid the effect of any coelution, the MS was operated in full-scan mode to identify a possible decomposition of the solute. The GC oven was programmed from 313 K (30 s) at 0.17 K·s^{-1} to 473 K (30 s) and then at 0.33 K·s^{-1} to 553 K (30 s).

Initial Testing of the Extraction Apparatus. The purpose of the test was to check whether the composition of the aqueous effluent from the cell corresponded to equilibrium between the solid PAH and the aqueous effluent from the cell. During the test, both length and diameter of the restrictor were varied to produce different flow rates of the aqueous solution at a fixed temperature and pressure in the extraction cell. The test was carried out with anthracene at 333 K and 5 MPa, and the mass flow rate of water varied within (0.007 to 0.030) g·s^{-1}. The results did not reveal any significant dependence of the composition of the aqueous effluent on the water flow rate. We assumed that the rate of equilibration between the solid PAH and the aqueous solution increased with increasing temperature of the extraction cell. In the measurements, therefore, the mass flow rate of water always ranged within the limits mentioned above.

Results and Discussion

Solubility Data. Table 1 shows the resultant solubilities (equilibrium mole fractions, x_2) of PAHs in water. In accordance with the previous reports,[22−26] a strong increase of solubility with raising temperature is apparent in all solutes. Unlike the previous reports, the solubilities were measured in narrow temperature intervals (20 K or less). The maximum temperature was (5 to 10) K below the triple-point temperature of the particular PAH. As regards the stability of PAHs in PHW, the analysis of the toluene extracts of the aqueous solutions did not indicate any noticeable decomposition of any of the PAHs investigated under the experimental conditions of our work. This result accords with the previous findings by others,[4] and it reflects the relatively low maximum temperature of this study (a temperature of 483 K) as well as the relatively large amounts of PAHs in the extraction cell. Recently, Andersson et al.[29] reported decomposition of PAHs in PHW when a small amount of PAH was spiked on sea sand in the extraction cell but did not observe a noticeable decomposition with larger amounts of PAHs in the later study[26] of PAH solubility in PHW. Consider-

Table 1. Aqueous Solubilities of PAHs (x_2) and Their Standard Deviations (SD) as Functions of Temperature (T) and Pressure (P)

PAH	T/K	P/MPa	$10^9 x_2$	10^9 SD^a
naphthalene	313.2	5.0	6920	132
	318.2	5.0	8600	160
	323.2	5.0	11400	157
	328.2	5.0	15500	743
	333.2	5.1	20700	1190
	338.2	5.1	26400	1090
	343.2	5.0	34800	907
	348.2	5.0	43500	1160
anthracene	313.2	5.0	11.9	0.54
	333.2	5.1	42.2	0.83
	353.2	5.0	137	5.3
	373.2	3.9	457	32
	393.2	5.2	1540	99
	413.2	4.7	5370	100
	433.2	5.4	15900	439
	453.2	6.3	48400	1210
	473.2	7.7	130000	2870
	483.2	5.5	220000	6740
1,2-benzanthracene	313.2	5.1	3.37	0.15
	333.2	5.0	8.46	0.27
	353.2	5.0	29.5	0.79
	373.2	5.0	113	3.2
	393.2	5.2	418	21
	413.2	4.9	1600	52
	423.2	4.9	2960	51
triphenylene	313.2	5.5	1.82	0.048
	333.2	5.1	6.07	0.031
	353.2	5.1	23.0	0.43
	373.2	5.1	89.9	2.6
	393.2	5.2	353	9.1
	413.2	5.0	1260	9.2
	433.2	5.5	3770	66
	453.2	6.4	12300	429
	463.2	6.4	23000	212
	468.2	6.0	28300	930
p-terphenyl	333.2	5.0	0.849	0.050
	353.2	4.9	3.85	0.21
	373.2	4.9	21.9	1.7
	393.2	4.9	90.0	0.78
	413.2	5.1	372	9.1
	433.2	6.7	1540	79
	453.2	5.5	6260	62
	473.2	5.3	24100	314
	483.2	5.4	39300	339

^{a} Standard deviations (SD) are based on five fractions collected at each condition.

ing the data in Table 1 and the standard uncertainties in temperature and pressure mentioned above, we conclude that the relative expanded uncertainty[28] in the resultant solubilities is ± 10 % (confidence level of 95 %).

Comparison of Solubility Data with Literature Values. The comparison of the present results with independent data can only be made in naphthalene and anthracene. To our knowledge, based on the literature search at the time of this writing, the solubilities in PHW of the other PAHs included in this work have been reported for the first time.

Table 2 shows a selection of literature data on aqueous solubility of naphthalene within the temperature range of this study. The data of Miller and Hawthorne[24] and the present results were measured at elevated pressures ((3 to 7) MPa) whereas the other sets[30−32] were low-pressure data. In the temperature range of (313 to 328) K, the low-pressure solubilities[30−32] exceed the present results, but the difference diminishes with increasing temperature. At the upper limit of the temperature range shown in Table 2, the present result is higher than the low-pressure value of Wauchope and Getzen.[30]

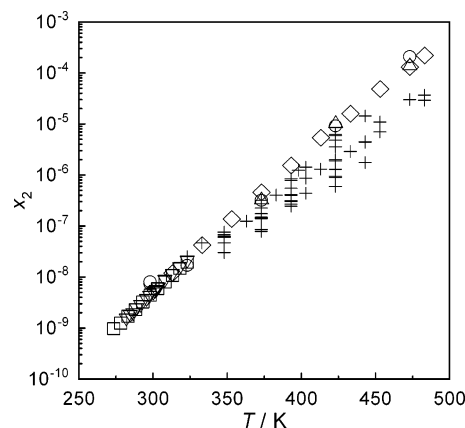**Table 2. Literature Data on Aqueous Solubilities of Naphthalene**

		$10^9 x_2$				
T/K	P/MPa	ref 30	ref 31	ref 32	ref 24	this work
312.45		7550				
312.45			7702			
313.15				7920		
313.2	5					6920
313.25		7790				
317.85		9400				
318.05			9684			
318.2	5					8600
323.15		11700				
323.15	7				14200	
323.2	5					11400
323.35		11800				
328.2	5					15500
328.75		15000				
333.2	5.1					20700
337.65		22400				
338.15	3				30400	
338.2	5.1					26400
343.2	5					34800
346.55		34400				
348.15		37200				
348.2	5					43500

Table 3. Literature Data on Aqueous Solubilities of Anthracene Measured by Variants of Dynamic Method

		$10^9 x_2$				
T/K	P/MPa	ref 25	ref 33	ref 34	ref 26	this work
313.06			11.7			
313.15				10.8		
313.2	5.0					11.9
318.05				15.9		
318.15				14.8		
323	5.0	17.0				
323.07				21.5		
323.15				19.5		
333.2	5.1					42.2
353.2	5.0					137
373	4.5	320				
373.2	3.9					457
373	5.0				325	
393.2	5.2					1540
413.2	4.7					5370
423	4.7	9200				
423	5.0				10200	
433.2	5.4					15900
453.2	6.3					48400
473	4.8	210000				
473.2	7.7					130000
473	5.0				138000	
483.2	5.5					220000

The solubilities reported by Miller and Hawthorne[24] exceed our results as well as the low-pressure data.

In Table 3, the present results for anthracene are compared with other solubility data measured by variants of dynamic method. The results of Miller et al.,[25] Reza et al.,[33] Dohányosová et al.,[34] and Andersson et al.[26] were all obtained by variants of dynamic saturation method, with the data of Miller et al.[25] and Andersson et al.[26] referring to elevated pressure ((4.5 to 5.0) MPa) and the data of Reza et al.[33] and Dohányosová et al.[34] referring to lower pressures (up to 1.5 MPa).[34] At the lower limit of the temperature range shown in Table 3, the present result is slightly higher than the low-pressure data.[33,34] At the temperature of 373.2 K, our value of anthracene solubility is by about 40 % higher than the data of Miller et al.[25] and Andersson et al.[26] At the temperature of 473.2 K, the present result is very close to the solubility value reported by Andersson et al.[26] and markedly (by about 62 %) lower than the value reported by Miller et al.[25] Despite these differences, the high-

Figure 2. Selected data on aqueous solubility of anthracene: ○, Miller et al.;[25] ▽, Reza et al.;[33] □, Dohányosová et al.;[34] △, Andersson et al.;[26] +, Rössling and Franck;[22] ◇, this work.

temperature data on aqueous solubility of anthracene measured by the dynamic saturation method are still relatively consistent when compared with the classical results obtained by Rössling and Franck[22] from UV spectrophotometry. Figure 2 shows a distinct disagreement between the spectrophotometric and the dynamic saturation data. The cause of the disagreement is not clear. The original data of Rössling and Franck[22] were reported as molarities (mol·L^{-1}). We converted the data to mole fractions assuming that the density of the anthracene solution was equal to the density of pure water at the particular temperature and pressure, with the density of pure water calculated from the IAPWS-95 equation of state of Wagner and Pruss.[35] Because of low solubility of anthracene even at the upper limit of temperature shown in Figure 2 and because of the 164-K temperature interval between the upper limit and the critical temperature of water, the possible errors introduced by the data conversion alone cannot explain the disagreement. Furthermore, although the pioneering study by Rössling and Franck[22] covered a very wide interval of pressure ((2 to 285) MPa), the effect of pressure also cannot explain the disagreement because even the part of Rössling and Franck's data measured at lower pressures (< 10 MPa) also deviate from the dynamic saturation results. Therefore, the most probable cause of the deviation seems to be the Rössling and Franck's presumption[22] of the temperature- and pressure-independent molar absorptivity of anthracene.

Variation of Solubility with Temperature. Simple linear fits of the data in Table 1 show that the mean values of the relative increase in solubility with temperature, $(\partial \ln x_2/\partial T)_\sigma$, are 0.054 K^{-1}, 0.058 K^{-1}, 0.063 K^{-1}, 0.063 K^{-1}, and 0.072 K^{-1} in naphthalene, anthracene, 1,2-benzanthracene, triphenylene, and p-terphenyl, respectively. A more detailed insight results from fitting the solubilities reported in Table 1 with

$$\ln x_2 = a_1 + a_2(T_0/T) + a_3 \ln(T/T_0) \quad (1)$$

where $T_0 = 298.15$ K. The coefficients a_1, a_2, and a_3 can be used to estimate the values of $RT^2(\partial \ln x_2/\partial T)_\sigma$ from

$$RT^2\left(\frac{\partial \ln x_2}{\partial T}\right)_\sigma = R(a_3 T - a_2 T_0) \quad (2)$$

where R is the molar gas constant, and the subscript σ denotes saturation. The least-squares estimates of the coefficients a_1, a_2, and a_3 are listed in Table 4. In all coefficients, the ratio of the coefficient estimate to the standard deviation of the coefficient estimate can be compared to the pertinent critical values of the Student's t distribution[36] to test the hypothesis

Table 4. Least-Squares Estimates of the Coefficients a_1, a_2, and a_3 of Equation 1 and the Standard Deviations (SD) of the Estimates, with T_{min} and T_{max} Indicating the Minimum and the Maximum Temperatures of the PAH Solubility Measurements, Respectively

solute	naphthalene[a]	anthracene	1,2-benz-anthracene	triphenylene	p-terphenyl
T_{min}/K	313.2	313.2	313.2	313.2	333.2
T_{max}/K	348.2	483.2	423.2	468.2	483.2
a_1	−17.39	−34.63	−75.51	−38.03	−34.11
SD of a_1	21.75	2.27	7.56	3.95	4.73
a_2	4.62	15.40	55.24	16.78	10.18
SD of a_2	21.84	2.32	7.66	4.03	4.88
a_3	22.01	34.68	68.30	37.49	36.78
SD of a_3	19.73	1.78	6.27	3.12	3.63

[a] Large SDs of the naphthalene parameters reflect the narrow temperature range available for the measurements with solid naphthalene.

Table 5. Values of $RT^2(\partial \ln x_2/\partial T)_\sigma$/kJ·mol^{-1} Calculated from Equation 2

T/K	naphthalene	anthracene	1,2-benz-anthracene	triphenylene	p-terphenyl
313.2	(45.9)	52.1	40.9	56.0	
333.2	(49.5)	57.9	52.2	62.2	76.6
353.2		63.7	63.6	68.5	82.8
373.2		69.4	74.9	74.7	88.9
393.2		75.2	86.3	80.9	95.0
413.2		81.0	97.7	87.2	101
433.2		86.7		93.4	107
453.2		92.5		99.7	113
473.2		98.3			119
483.2		101			123

"the coefficient equals zero". Except for the coefficients of naphthalene, the hypothesis is rejected at a confidence level of 98 %, indicating that most coefficients are statistically significant. The values of $RT^2(\partial \ln x_2/\partial T)_\sigma$ estimated from eq 2 are compiled in Table 5. The entries for naphthalene are given in parentheses because, as a result of the narrow temperature interval available for the measurements with solid naphthalene, the respective coefficients a_1, a_2, and a_3 are not statistically significant.

The temperature dependence of solubility has often been used to estimate the enthalpy of solution. However, the temperature derivative of solubility alone is not sufficient for the purpose. Employing standard thermodynamic relationships,[37,38] one can write the following sequence of equations for the isobaric temperature derivative of solubility (= equilibrium mole fraction):

$$\left(\frac{\partial \ln x_2}{\partial T}\right)_{P,\sigma} = \left(\frac{\partial \ln f_2^{s0}}{\partial T}\right)_P - \left(\frac{\partial \ln f_2^{l0}}{\partial T}\right)_P - \left(\frac{\partial \ln \gamma_2}{\partial T}\right)_{P,\sigma} \quad (3)$$

$$\left(\frac{\partial \ln x_2}{\partial T}\right)_{P,\sigma} = \frac{h_2^{*0} - h_2^{s0}}{RT^2} - \frac{h_2^{*0} - h_2^{l0}}{RT^2} + \frac{\bar{h}_2 - h_2^{l0}}{RT^2} -$$
$$\left(\frac{\partial \ln \gamma_2}{\partial \ln x_2}\right)_{T,P}\left(\frac{\partial \ln x_2}{\partial T}\right)_{P,\sigma} \quad (4)$$

$$\left(\frac{\partial \ln x_2}{\partial T}\right)_{P,\sigma} = \left\{\frac{\bar{h}_2 - h_2^{s0}}{RT^2}\right\}\Bigg/\left\{\left[1 + \left(\frac{\partial \ln \gamma_2}{\partial \ln x_2}\right)_{T,P}\right]\right\} \quad (5)$$

where P is the pressure, f_2^{s0} is the fugacity of the pure solid solute, f_2^{l0} is the fugacity of the pure solute in the state of subcooled liquid, γ_2 is the Raoult law activity coefficient of the solute referred to the pure subcooled liquid solute at the particular T and P, h_2^{*0} is the molar enthalpy of the pure solute in the ideal-gas state, h_2^{s0} is the molar enthalpy of the pure solid
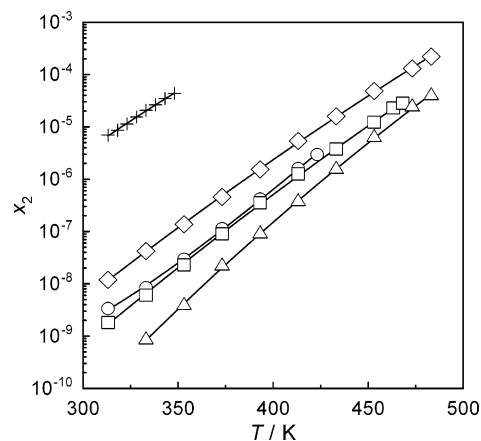

Figure 3. Experimental data on PAH solubility vs equation 1: +, naphthalene; ◇, anthracene; ○, 1,2-benzanthracene; □, triphenylene; △, p-terphenyl. The lines show the best fits with eq 1.

solute, h_2^{l0} is the molar enthalpy of the pure subcooled liquid solute, and $\bar{h}_2$ is the partial molar enthalpy of the solute in the aqueous solution. Equation 5 indicates that the derivative $(\partial \ln x_2/\partial T)_{P,\sigma}$ cannot be converted to the transfer enthalpy $\bar{h}_2 - h_2^{s0}$ unless the quotient $(\partial \ln \gamma_2/\partial \ln x_2)_{T,P}$ is known. In highly nonideal water (1) + PAH (2) systems, the limiting value $(x_2 \rightarrow 0)$ of the derivative $(\partial \ln \gamma_2/\partial \ln x_2)_{T,P}$ is likely to be significantly different from zero. Therefore, because of the denominator term on the right-hand side of eq 5, the values of $RT^2(\partial \ln x_2/\partial T)_\sigma$ in Table 4 would not be equal to the transfer enthalpies $\bar{h}_2 - h_2^{s0}$ even if the measurements were strictly isobaric.

The fits of the data from Table 1 with eq 1 are shown in Figure 3 indicating different signs of curvature in the $\ln x_2$ versus T plots of the individual PAHs. While $(\partial^2 \ln x_2/\partial T^2)_\sigma < 0$ in the plots of anthracene, triphenylene, and p-terphenyl, the plot of 1,2-benzanthracene shows an opposite curvature with $(\partial^2 \ln x_2/\partial T^2)_\sigma > 0$. It should be noted that the different signs of curvature are not an artifact of eq 1 used for fitting. The different signs of curvature are apparent when drawing straight lines between the data points at the limits of the temperature range in the individual PAHs. Because of the logarithmic scale on the vertical axis of Figure 3 and because of the fact that the solubilities of the individual PAHs span over 3 or more orders of magnitude, the different signs of curvature are even invariant with respect to the relative expanded uncertainty in the solubility data given above. Although the uncertainty in the data definitely precludes any quantitative conclusions based on curvature of the plots, a qualitative explanation of the difference between the plots of 1,2-benzanthracene and of the other PAHs is needed.

From eq 4, one obtains the following expression for $(\partial^2 \ln x_2/\partial T^2)_{P,\sigma}$:

$$(\partial^2 \ln x_2/\partial T^2)_{P,\sigma} = (A + B)/C \quad (6)$$

with

$$A = \frac{1}{RT^2}\left[\bar{c}_{P2} - c_{P2}^{s0} - \frac{2}{T}(\bar{h}_2 - h_2^{s0})\right]$$

$$B = \frac{2}{RT^2}\left(\frac{\partial \bar{h}_2}{\partial \ln x_2}\right)_{T,P}\left(\frac{\partial \ln x_2}{\partial T}\right)_{P,\sigma} - \left(\frac{\partial^2 \ln \gamma_2}{\partial (\ln x_2)^2}\right)_{T,P}\left(\frac{\partial \ln x_2}{\partial T}\right)_{P,\sigma}^2$$

$$C = 1 + 2\left(\frac{\partial \ln \gamma_2}{\partial \ln x_2}\right)_{T,P}$$

where c_{P2}^{s0} is the molar isobaric heat capacity of the pure solid solute, and $\bar{c}_{P2}$ is the partial molar isobaric heat capacity of the solute in the aqueous solution.

Equation 6 consists of a number of difficult to estimate terms and, therefore, provides little clue to determine the sign of $(\partial^2 \ln x_2/\partial T^2)_{P,\sigma}$ in a particular water (1) + PAH (2) system. However, the different signs of curvature may reflect the evident structural difference among the PAH molecules concerned. Unlike the molecules of anthracene, triphenylene, and *p*-terphenyl, the 1,2-benzanthracene molecule has neither center of symmetry nor axis of symmetry. The lack of symmetry in the PAH molecule is likely to make the water + 1,2-benzanthracene interaction distinctly different from those in the other water + PAH systems, with concomitant effects on the terms in eq 6 containing $\bar{c}_{P2}$, $\bar{h}_2$, and γ_2.

Conclusions

A dynamic method with a flow-through extraction cell was employed to measure the solubilities (mole fractions, x_2) of several solid PAHs in pressurized hot water within 313 K to the PAH melting point in relatively narrow temperature increments (20 K or less). Care was taken to minimize the system volume downstream of the sampling point. The narrow temperature increments together with the particular experimental arrangement made it possible to observe the curvature of the ln x_2 versus T plots. The curvature of the plot for 1,2-benzanthracene was opposite to that observed in anthracene, triphenylene, and *p*-terphenyl. The uncertainty in the solubility data was too high to allow any quantitative interpretation of the curvature of the plots. Nevertheless, the present results suggest that the sign of curvature of a ln x_2 versus T plot (i.e., the sign of $(\partial^2 \ln x_2/\partial T^2)_\sigma$) can be qualitatively associated with symmetry of the PAH molecule concerned.

The previous attempts to correlate the aqueous solubilities of PAHs at elevated temperature and pressure were limited to simple relations describing the solubilities of individual PAHs as functions of temperature.[25,26] In the conclusion of their pioneering work on the use of dynamic method to measure the PAH solubilities in pressurized hot water, Miller et al.[25] noted that more experimental data will be needed to refine the correlations for aqueous solubility of PAHs. The present study extends the database of PAH solubilities in pressurized hot water by providing the first results reported for 1,2-benzanthracene, triphenylene, and *p*-terphenyl. In a subsequent contribution, we will use the available data to develop a more general correlation of the PAH solubilities in pressurized hot water.

Literature Cited

(1) Shaw, R. W.; Brill, T. B.; Clifford, A. A.; Eckert, C. A.; Franck, E. U. Supercritical water: a medium for chemistry. *Chem. Eng. News* **1991**, *69*, 26−39.

(2) Savage, P. E. Organic chemical reactions in supercritical water. *Chem. Rev.* **1999**, *99*, 603−621.

(3) Siskin, M.; Katritzky, A. R. Reactivity of organic compounds in superheated water: general background. *Chem. Rev.* **2001**, *101*, 825−835.

(4) Katritzky, A. R.; Nichols, D. A.; Siskin, M.; Murugan, R.; Balasubramanian, M. Reactions in high-temperature aqueous media. *Chem. Rev.* **2001**, *101*, 837−892.

(5) Palmer, D. A., Fernández-Prini, R., Harvey, A. H., Eds. *Aqueous Systems at Elevated Temperatures and Pressures. Physical Chemistry in Water, Steam and Hydrothermal Solutions*; Elsevier−Academic Press: London, UK, 2004.

(6) Weingärtner, H.; Franck, E. U. Supercritical water as a solvent. *Angew. Chem., Int. Ed.* **2005**, *44*, 2672−2692.

(7) Hawthorne, S. B.; Yang, Y.; Miller, D. J. Extraction of organic pollutants from environmental solids with sub- and supercritical water. *Anal. Chem.* **1994**, *66*, 2912−2920.

(8) Ramos, L.; Kristenson, E. M.; Brinkman, U. A. T. Current use of pressurised liquid extraction and subcritical water extraction in environmental analysis. *J. Chromatogr. A* **2002**, *975*, 3−29.

(9) Smith, R. M. Extractions with superheated water. *J. Chromatogr. A* **2002**, *975*, 31−46.

(10) Carabias-Martínez, R.; Rodríguez-Gonzalo, E.; Revilla-Ruiz, P.; Hernández-Méndez, J. Pressurized liquid extraction in the analysis of food and biological samples. *J. Chromatogr. A* **2005**, *1089*, 1−17.

(11) Coym, J. W.; Dorsey, J. G. Superheated water chromatography: a brief review of an emerging technique. *Anal. Lett.* **2004**, *37*, 1013−1023.

(12) Lagadec, A. J. M.; Miller, D. J.; Lilke, A. V.; Hawthorne, S. B. Pilot-scale subcritical water remediation of polycyclic aromatic hydrocarbon- and pesticide-contaminated soil. *Environ. Sci. Technol.* **2000**, *34*, 1542−1548.

(13) Kubátová, A.; Lagadec, A. J. M.; Hawthorne, S. B. Dechlorination of lindane, dieldrin, tetrachloroethane, trichloroethene, and PVC in subcritical water. *Environ. Sci. Technol.* **2002**, *36*, 1337−1343.

(14) Kubátová, A.; Herman, J.; Steckler, T. S.; de Veij, M.; Miller, D. J.; Klunder, E. B.; Wai, C. M.; Hawthorne, S. B. Subcritical (hot/liquid) water dechlorination of PCBs (Aroclor 1254) with metal additives and in waste paint. *Environ. Sci. Technol.* **2003**, *37*, 5757−5762.

(15) Basile, A.; Jiménez-Carmona, M. M.; Clifford, A. A. Extraction of rosemary by superheated water. *J. Agric. Food Chem.* **1998**, *46*, 5205−5209.

(16) Rovio, S.; Hartonen, K.; Holm, Y.; Hiltunen, R.; Riekkola, M.-L. Extraction of clove using pressurized hot water. *Flavour Fragrance J.* **1999**, *14*, 399−404.

(17) Kubátová, A.; Lagadec, A. J. M.; Miller, D. J.; Hawthorne, S. B.: Selective extraction of oxygenates from savory and peppermint using subcritical water. *Flavour Fragrance J.* **2001**, *16*, 64−73.

(18) Yang, Y.; Miller, D. J.; Hawthorne, S. B. Toluene solubility in water and organic partitioning from gasoline and diesel fuel into water at elevated temperatures and pressures. *J. Chem. Eng. Data* **1997**, *42*, 908−913.

(19) Miller, D. J.; Hawthorne, S. B. Solubility of liquid organics of environmental interest in subcritical (hot/liquid) water from 298 K to 473 K. *J. Chem. Eng. Data* **2000**, *45*, 78−81.

(20) Miller, D. J.; Hawthorne, S. B. Solubility of liquid organic flavor and fragrance compounds in subcritical (hot/liquid) water from 298 K to 473 K. *J. Chem. Eng. Data* **2000**, *45*, 315−318.

(21) Mathis, J.; Gizir, A. M.; Yang, Y. Solubility of alkylbenzenes and a model for predicting the solubility of liquid organics in high-temperature water. *J. Chem. Eng. Data* **2004**, *49*, 1269−1272.

(22) Rössling, G. L.; Franck, E. U. Solubility of anthracene in dense gases and liquids to 200 °C and 2000 bar. *Ber. Bunsen-Ges. Phys. Chem.* **1983**, *87*, 882−890.

(23) Sanders, N. D. Visual observation of the solubility of heavy hydrocarbons in near-critical water. *Ind. Eng. Chem. Fundam.* **1986**, *25*, 169−171.

(24) Miller, D. J.; Hawthorne, S. B. Method for determining the solubilities of hydrophobic organics in subcritical water. *Anal. Chem.* **1998**, *70*, 1618−1621.

(25) Miller, D. J.; Hawthorne, S. B.; Gizir, A. M.; Clifford, A. A. Solubility of polycyclic aromatic hydrocarbons in subcritical water from 298 K to 498 K. *J. Chem. Eng. Data* **1998**, *43*, 1043−1047.

(26) Andersson, T. A.; Hartonen, K. M.; Riekkola, M.-L. Solubility of acenaphthene, anthracene, and pyrene in water at 50 °C to 300 °C. *J. Chem. Eng. Data* **2005**, *50*, 1177−1183.

(27) Krammer, P.; Vogel, H. Hydrolysis of esters in subcritical and supercritical water. *J. Supercrit. Fluids* **2000**, *16*, 189−206.

(28) Chirico, R. D.; Frenkel, M.; Diky, V. V.; Marsh, K. N.; Wilhoit, R. C. ThermoML—an XML-based approach for storage and exchange of experimental and critically evaluated thermophysical and thermochemical property data. 2. Uncertainties. *J. Chem. Eng. Data* **2003**, *48*, 1344−1359.

(29) Andersson, T.; Hartonen, K.; Hyötyläinen, T.; Riekkola, M.-L. Stability of polycyclic aromatic hydrocarbons in pressurized hot water. *Analyst* **2003**, *128*, 150−155.

(30) Wauchope, R. D.; Getzen, F. W. Temperature dependence of solubilities in water and heats of fusion of solid aromatic hydrocarbons. *J. Chem. Eng. Data* **1972**, *17*, 38−41.

(31) Bennett, D.; Canady, W. J. Thermodynamics of solution of naphthalene in various water−ethanol mixtures. *J. Am. Chem. Soc.* **1984**, *106*, 6, 910−915.

(32) Pérez-Tejeda, P.; Yanes, C.; Maestre, A. Solubility of naphthalene in water + alcohol solutions at various temperatures. *J. Chem. Eng. Data* **1990**, *35*, 244−246.

(33) Reza, J.; Trejo, A.; Vera-Ávila, L. E. Determination of the temperature dependence of water solubilities of polycyclic aromatic hydrocarbons by a generator-column-on-line solid-phase extraction-liquid chromatographic method. *Chemosphere* **2002**, *47*, 933−945.

(34) Dohányosová, P.; Dohnal, V.; Fenclová, D. Temperature dependence of aqueous solubility of anthracenes. *Fluid Phase Equilib.* **2003**, *214*, 151−167.

(35) Wagner, W.; Pruss, A. The IAPWS formulation 1995 for the thermodynamic properties of ordinary water substance for general and scientific use. *J. Phys. Chem. Ref. Data* **2002**, *31*, 387−535.

(36) Electronic Statistics Textbook. StatSoft, Inc., Tulsa, OK, 1999; http://www.statsoft.com/textbook/stathome.html.

(37) Tester, J. W.; Modell, M. *Thermodynamics and Its Applications*; Prentice Hall: Upper Saddle River, NJ, 1997; Chapter 9, pp 318−387.

(38) Prausnitz, J. M.; Lichtenthaler, R. N.; Gomes de Azevedo, E. *Molecular Thermodynamics of Fluid-Phase Equilibria*; Prentice Hall: Upper Saddle River, NJ, 1999; Chapter 6, pp 213−305.